Wind-Driven Circulation in the Chesapeake Bay, Winter 1975

DONG-PING WANG

Chesapeake Bay Institute, The Johns Hopkins University, Baltimore MD 21218

(Manuscript received 31 July 1978, in final form 18 December 1978)

ABSTRACT

Nontidal circulation in Chesapeake Bay was examined from one-month current records at 50 and 200 km from the entrance. The monthly mean flow was basically a two-layered circulation; in addition, there were large wind-driven velocity fluctuations at several-day time scales. Corresponding to velocity changes, the salinity distribution had large variations, comparable to its seasonal change.

Bay water responded to longitudinal (local) wind and coastal (nonlocal) Ekman flux. The response was barotropic in the lower Bay, and baroclinic (frictional) in the upper Bay. The difference in response characteristic appears to be due to the counter-effects of the near-surface windstress shear and the depth-independent surface slope. A frictional model accounts for most of the observed features.

Results of this study provide further evidence of large, atmospherically induced exchange between the estuary and coastal ocean. The importance of wind on upstream salt intrusions is also clearly demonstrated.

1. Introduction

Nontidal (tidally averaged) circulation in a partially mixed estuary was first studied by Pritchard (1952, 1956) in the James River. Pritchard identified a two-layered circulation pattern, with a landward flow in the lower layer and a seaward flow in the upper layer. The two-layered circulation is driven by the longitudinal salinity (density) gradient, and it is generally regarded as the basic flow pattern in a partially mixed estuary.

Nontidal circulation driven by wind forcing was examined by Weisberg (1976), who found high coherence between bottom current and longitudinal wind in the Providence River. The bottom currents were out-of-phase with winds, i.e., a seaward near-bottom flow was driven by an up-river wind, which suggests a baroclinic response. Wind-driven flow was comparable to the gravitational circulation as reversals of bottom landward flow were found during strong up-river winds. A baroclinic response to longitudinal wind forcing was also found in the Potomac River (Elliott, 1978), where the bottom flow reversed about every 2–3 days.

In addition to local wind forcing, nontidal current can be induced by nonlocal effects due to interaction with a larger, neighboring estuary or coastal ocean. Elliott (1978) found that a significant portion of the near-surface flow in the Potomac was due to the exchange with Chesapeake Bay proper. Evidence for the nonlocal coastal ocean effect was reported by Wang and Elliott (1978), who found high coherence between the subtidal sea level fluctuation in the Bay and coastal Ekman flux. The response of Bay water to wind forcing was frequency-dependent; it was local for time scales <3 days, and was nonlocal for time scales >10 days. Atmospherically induced exchange between estuary and coastal ocean was also found in Corpus Christi Bay, Texas (Smith, 1977).

In this study, the circulation pattern in the Chesapeake Bay proper is examined over a one-month period at two locations, 50 and 200 km from the entrance. A frictional model is developed to explain the key response characteristics. The purpose is to further document the wind-driven circulation in the Chesapeake Bay, and to assess the effects of wind forcing on salinity distributions.

2. Currents, salinity and wind forcing

a. Observations

Two moorings were maintained in the lower and upper Bay (Fig. 1) over a one-month period (19 November to 20 December 1975). The lower Bay mooring had two current meters at depths of 4 m (13 ft) and 7.8 m (26 ft) in a water depth of 12 m. The upper Bay mooring had two currents meters at depths of 4.5 m (15 ft) and 9 m (30 ft), in a water depth of 14 m. For both moorings, the top current meter was an Endeco 105, and the bottom meter was an Aanderaa (which also recorded temperature and conductivity). Data were low-pass filtered to remove the diurnal and semidiurnal tides and other high-frequency fluctuations. [The low-pass signals

0022-3670/79/030564-09$06.25

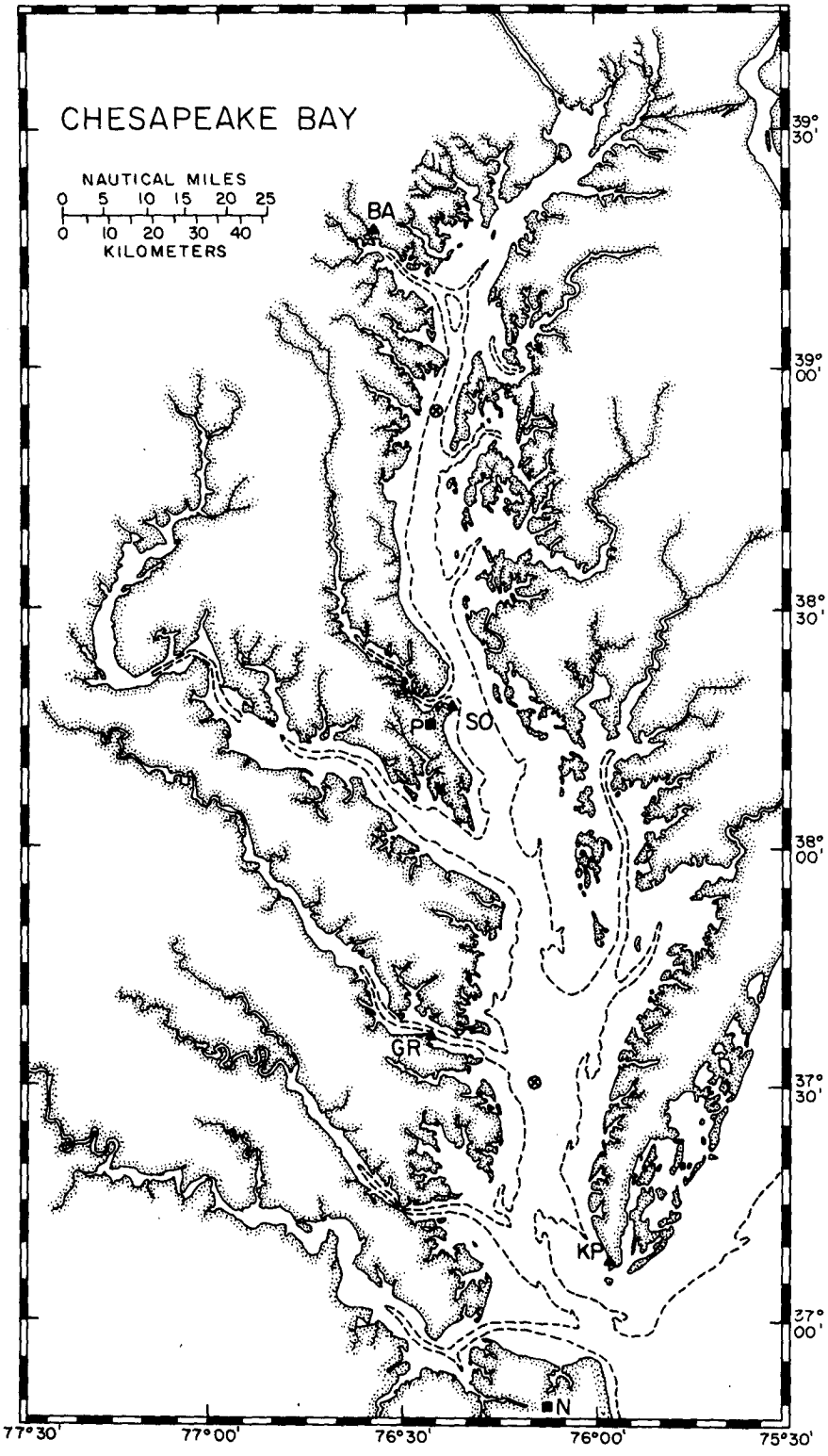

FIG. 1. Map of the Chesapeake Bay showing the 9 m depth contour (dashed) and wind (■), sea level (▲) and current meter (⊗) stations.

have nil amplitude at 1 cpd (cycle per day), half-amplitude at 0.7 cpd, and 95% amplitude at 0.5 cpd.] The resulting series were then decimated to 6 h values.

The velocity was decomposed into longitudinal (principal axis) and lateral components. However, the weak, lateral component (~5% of the total variance) was not included in the analysis, as it was subject to large uncertainties due to compass error. Due to instrument malfunction, the lower Bay bottom meter record had a one-week data gap.

Sea levels were obtained at Kiptopeake Beach, Grey Pt., Solomons I. and Baltimore (Fig. 1). The low-pass sea levels were similar among Bay stations, and therefore, only Solomons I. (Bay station) and Kiptopeake Beach (coastal station) records are shown in Fig. 2. The volume transport (Fig. 2) at the lower Bay mooring section was computed from upstream sea level variations, based on the continuity requirement. Fig. 2 also shows the sea level difference between Baltimore and Kiptopeake Beach.

Wind records were obtained at Patuxent River and Norfolk (Fig. 1), and stresses were computed from the quadratic drag law ($C_D = 2.5 \times 10^{-3}$). The low-pass wind (windstress) fluctuations were mainly in north–south directions (Fig. 2), and were coherent between the two stations ($\gamma^2 = 0.75$); however, the Norfolk wind was considerably stronger. The north–south wind was highly coherent with the surface slope along the Bay ($\gamma^2 = 0.82$), which indicates a simple wind set-up relation.

b. Velocity and salinity

In the lower Bay, the monthly mean flow was 10.3 cm s^{-1} seaward near surface and 5.0 cm s^{-1} landward near bottom, which is consistent with the gravitational circulation pattern. Velocity fluctuations, predominantly at time scales of 2 to 7 days, were apparently coherent and in-phase between the two depths (Fig. 3). To examine the cross-sectional homogeneity, the observed velocity was compared with the volume transport. The sectional mean flow (volume transport divided by the cross-section area) was highly coherent with the near-surface velocity fluctuation ($\gamma^2 = 0.8$), and their amplitudes were comparable. (The rms amplitude was 10 cm s^{-1} for both the sectional mean flow and near-bottom current, and 15 cm s^{-1} for the near-surface current.) Thus, the nontidal current in the lower Bay was basically a barotropic motion at the several-day time scales.

In the upper Bay, the monthly mean flow was 9.2 cm s^{-1} seaward near surface, and 2.5 cm s^{-1} landward near bottom which was comparable to the mean circulation in the lower Bay. The velocity fluctuations were coherent between the two depths; however, there was considerable phase difference particularly in the first part of the record. The near-bottom current generally led the near-surface current by 90°, i.e., the rate of change of the near-bottom current was large when the near-surface current reached an extreme. [A similar vertical phase difference was found in the Potomac River (Wang and Elliott, 1978).] The rms amplitudes of near-surface and near-bottom current were 11.4 and 7.6 cm s^{-1}, respectively. And, they were considerably larger than the sectional mean flow of 4.9 cm s^{-1}. Thus, due to their vertical phase difference, currents in the upper Bay had large baroclinic fluctuations.

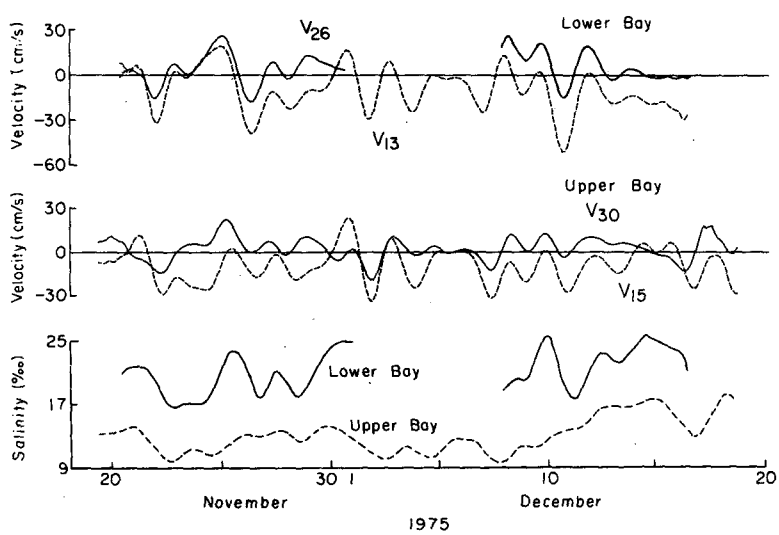

FIG. 2. The low-pass time series of lower Bay current at 13 (V_{13}) and 26 (V_{26}) ft below the surface (top panel), upper Bay current at 15 (V_{15}) and 30 (V_{30}) ft below the surface (middle panel) and near-bottom salinity in the lower and upper Bay (bottom panel).

Near-bottom salinity in the lower Bay had large variations (~2.0‰), which appeared to be induced by variations of the near-bottom current. For example, the sudden salinity decreases on 22 and 26 November and 10 December were associated with reversals of the near-bottom current (Fig. 3). And, the salinity increases on 24 November and 9 December were associated with a strong landward flow.

Near-bottom salinity in the upper Bay had similarly large variations (~1.9‰), which were also related to changes of the near-bottom current. For example, the sudden salinity decreases on 22 No-

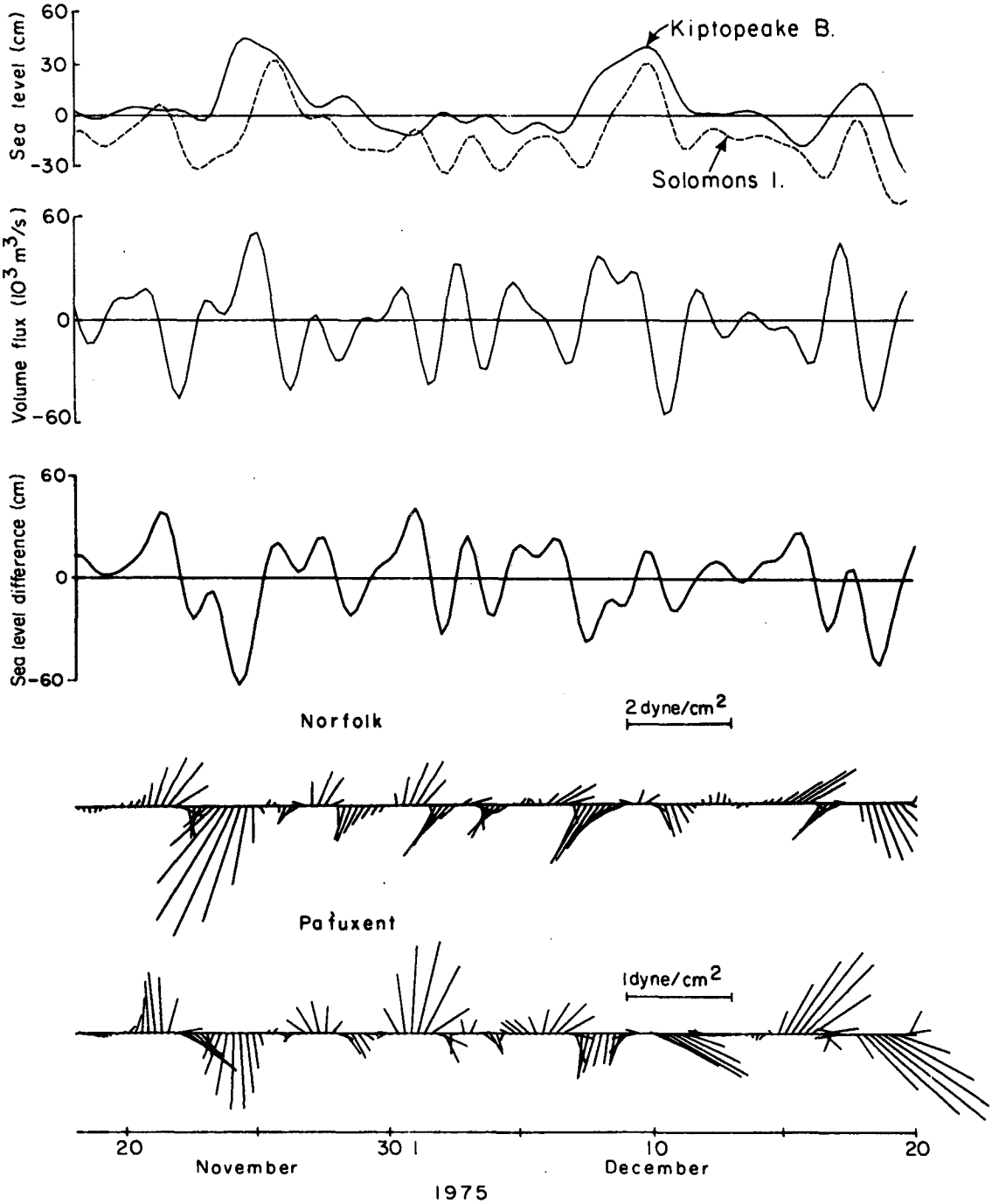

FIG. 3. The low-pass time series of (a) sea level at Solomons I. and Kiptopeake B., (b) volume flux at the lower Bay mooring section, (c) sea level difference between Baltimore and Kiptopeake B., and (d) wind at Patuxent River and Norfolk.

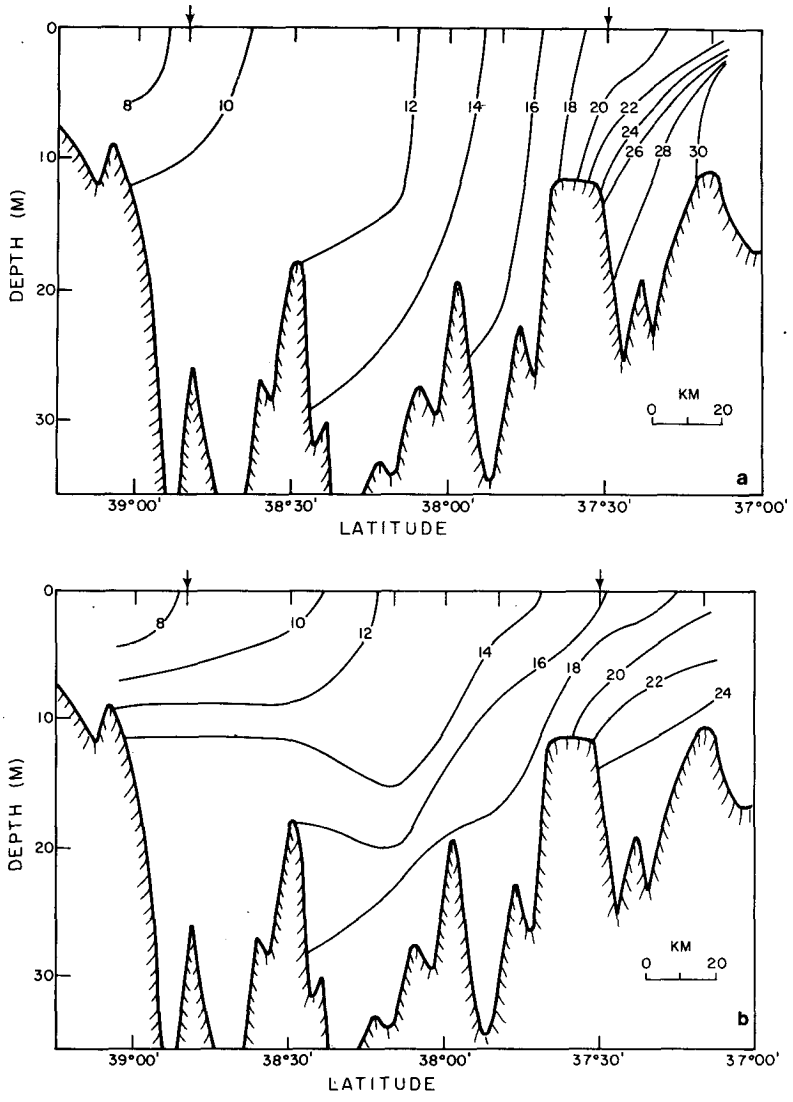

FIG. 4. Salinity section (‰) along the Bay axis (The mooring locations are marked by an arrow): (a) 9 December 1975, (b) 11–12 December 1975.

vember, and 1 and 15 December were associated with reversals of near-bottom current (Fig. 3). And, the salinity increases from 8–15 December were due to a persistent landward flow.

Two salinity slack runs were made on 9 December and 11–12 December along the Bay axis (Figs. 4a and 4b). (A slack run section is constructed using data collected on a single day run along the axis of the Bay, following as closely as possible the motion of the slack-before-flood point on a single tidal cycle as it progresses from the entrance to the head of the Bay. The procedure yields a salinity section having minimal distortion from tidal effects.) The abrupt salinity decrease in the lower Bay, within 70 km from the entrance, was associated with a strong seaward flow on 10 December (Fig. 3). In the mid- and upper Bay, salinities in the upper layer also decreased as a result of the same outflow event. In contrast, salinities in the lower layer increased significantly from 9 to 12 December due to a persistent landward flow (Fig. 3). Thus, large changes in salinity and stratification over the entire Bay occurred within a few days, due to changes in the nontidal circulation.

c. Wind forcing

Sea level and longitudinal wind were coherent and in-phase at time scales of 2–3 days. The amplitude of sea level increased towards the head of the Bay at these time scales. On the other hand, sea levels and longitudinal winds were out-of-phase at longer time scales. These results were similar to those of Wang and Elliott (1978), which suggested that sea level fluctuations were seiches driven by the longitu-

dinal wind at 2–3 day time scales, and were forced by the coastal Ekman flux at longer time scales. The nonlocal effect was evident during the two major events on 23–26 November and 7–10 December (Fig. 3). During both events, rapid rise of sea level was induced by a southward wind, through an onshore Ekman flux.

The volume transport was coherent and 90° out-of-phase with the sea level fluctuation. It had large amplitude in the lower Bay; for example, at the mooring section (50 km from the entrance), the rms amplitude was 23 000 $m^3 s^{-1}$, and the peak transport was 60 000 $m^3 s^{-1}$ (Fig. 3). For comparison, the total river runoff into the bay was only 1 000 $m^3 s^{-1}$. Thus, due to wind forcing, there was a large exchange of waters between the Bay and coastal ocean.

In the lower Bay, the velocity fluctuations were mainly barotropic, and can therefore be related to sea level change. Currents at time scales of 2–3 days were driven by longitudinal wind with a 90° phase difference, i.e., a strong landward (seaward) flow occurred at the onset of a northward (southward) wind. A quadrature phase relation is to be expected for a barotropic response, because the current is counterbalanced by the surface slope which is in-phase with the wind. For nonlocal forcing, current and wind usually were 180° out-of-phase, consistent with the coastal Ekman effect.

In the upper Bay, currents had large shear fluctuations which suggests a different forcing mechanism. Nearsurface current was highly coherent and in-phase with the longitudinal wind at all time scales ($\gamma^2 = 0.79$). In other words, a strong landward (seaward) flow occurred at the peak of a northward (southward) wind. The high correlation between wind and nearsurface current suggests frictional coupling, i.e., the nearsurface current was generated locally by the longitudinal wind. Nearbottom current, on the other hand, appeared to be also affected by the sea level change, particularly in the first part of the record when it led the nearsurface current (and, wind) by 90°.

3. Model interpretation

Our study indicates a barotropic response in the lower Bay, and a baroclinic response in the upper Bay. For example, the near-surface current was in-phase with the local wind in the upper Bay, but it led the wind by 90° in the lower Bay. The direct wind coupling in the upper Bay can be explained by the frictional effect. However, the quadrature phase relation in the lower Bay apparently contradicts the frictional coupling. On the other hand, our analysis indicates the existence of a large surface slope which counters the direct wind forcing. Being a semi-enclosed water body may be the main cause for barotropic response in the estuary.

A simple (conceptual) model is constructed to examine the estuarine response to longitudinal wind forcing. We assume the vertical dissipation as the dominant process. For a rectangular channel, the equations of motion for homogeneous water are

$$\frac{\partial u}{\partial t} = -g\frac{\partial \eta}{\partial x} + A_v\frac{\partial^2 u}{\partial z^2}, \tag{1}$$

$$\frac{\partial u}{\partial x} + \frac{\partial w}{\partial z} = 0, \tag{2}$$

where u and w are the longitudinal and vertical velocity, respectively, η the surface elevation and A_v a constant vertical eddy viscosity.

The boundary conditions are as follows.

(a) at the mouth, the elevation is constant;

$$x = 0: \quad \eta = 0$$

(b) at the head, the total transport is zero;

$$x = L: \quad U = 0$$

(c) at the surface, the shear is due to windstress;

$$z = 0: \quad A_v\frac{\partial u}{\partial z} = \tau_s$$

(d) at the bottom, the friction is proportional to the transport;

$$z = -H: \quad A_v\frac{\partial u}{\partial z} = \alpha\frac{U}{H}.$$

Here α is a linear drag coefficient.

The first three boundary conditions are standard. The choice of the bottom boundary condition becomes obvious, if the equations of motion are vertically integrated:

$$\begin{cases} \dfrac{\partial U}{\partial t} = -gH\dfrac{\partial \eta}{\partial x} + \tau_s - \dfrac{\alpha}{H}U, & (3) \\ \dfrac{\partial U}{\partial x} + \dfrac{\partial \eta}{\partial t} = 0. & (4) \end{cases}$$

Thus, the bottom boundary condition represents a simple overall friction damping. Since the friction does occur along the sidewall in a real estuary, we feel the friction damping is better modeled by the transport than the bottom velocity.

It is instructive (and simpler) to solve Eqs. (1) and (2), and Eqs. (3) and (4), by assuming an oscillating wind stress, i.e., $\tau_s \sim \exp(i\omega t)$, where ω is the angular frequency. The solutions are (apart from a common time oscillation factor)

$$\eta = \frac{1}{K\cos KL}\frac{\tau_s}{gH}\sin Kx,$$

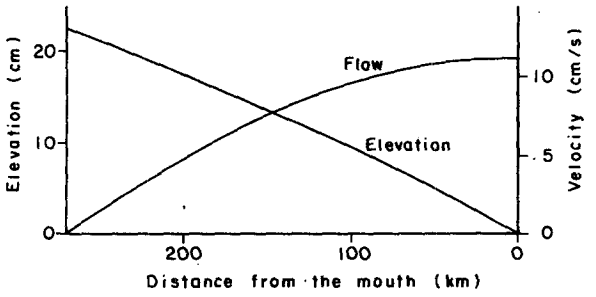

FIG. 5. Longitudinal distribution of sea level and sectional mean flow, from model computation.

$$\frac{\partial \eta}{\partial x} = \frac{1}{\cos KL}\frac{\tau_s}{gH}\cos Kx,$$

$$U = \frac{i\omega}{K^2 \cos KL}\frac{\tau_s}{gH}(\cos Kx - \cos KL),$$

and

$$u \equiv u_F + u_s,$$

$$u_F = \frac{-1}{\sinh(lH)}\frac{1}{l}\left\{\frac{\alpha}{A_v}\frac{U}{H} \times \cosh(lz) - \frac{\tau_s}{A_v}\cosh[l(H+z)]\right\},$$

$$u_s = \frac{i}{\omega}\frac{\tau_s}{H}\frac{\cos Kx}{\cos KL},$$

where

$$K^2 = \frac{1}{gH}\left(\omega^2 - i\omega\frac{\alpha}{H}\right),$$

$$l^2 = i\frac{\omega}{A_v},$$

are squares of the effective horizontal and vertical wavelength, respectively.

For a modestly dissipative estuary, surface slope and elevation are almost in-phase, and the transport is 90° out-of-phase with the windstress, which is consistent with the observations. The velocity consists of two components: the frictional part (u_F), due to the windstress and bottom dissipation, and the slope part (u_s), due to the surface slope. This becomes clear if we compute their respective transport:

$$U_F = -\frac{i}{\omega}\left(\tau_s - \frac{\alpha}{H}U\right), \quad U_s = \frac{i}{\omega}gH\frac{\partial \eta}{\partial x}.$$

Since the total transport (U) is small in the upper Bay, one expects large wind-driven frictional transport. On the other hand, the windstress contribution is less significant in the lower Bay where the total transport is large. These results seem to explain the apparent absence of wind-driven frictional response in the lower Bay.

To have a better understanding of the nature of estuarine response, a numerical example is computed. The following parameters are chosen, corresponding to "averaged" Chesapeake Bay conditions:

$L = 270$ km
$H = 8.4$ m
$\omega = 3 \times 10^{-5}$ s^{-1} (or 2.5 days)
$A_v = 10$ cm^2 s^{-1},
$\alpha = 10^{-2}$ cm s^{-1} (or decay time $\sim$ 1 day),
$\tau_s = 0.5$ dyn cm^{-2}.

Surface elevations increase linearly toward the head (Fig. 5), and they lag the surface wind by about 10°. Volume transports decrease linearly toward the head (Fig. 5), and they lead the surface wind by about 80°. The velocity profile varies considerably from the head to the mouth. In the upper Bay, a strong near-surface current is almost in-phase with the surface wind (Fig. 6). There is also a near-bottom return flow which partially compensates for the near-surface wind-driven flow. The sectional mean flow is 4 cm s^{-1}, which is considerably less than the nearsurface current (velocity averaged over the top 2 m is 10 cm s^{-1}). It is also noted that the near-bottom return flow leads the near-surface flow by about 90°. In the lower Bay, velocities are rather homogeneous (Fig. 6). The sectional mean flow of 11 cm s^{-1} is comparable to the nearsurface current (velocity averaged over the top 2 m is 16 cm s^{-1}). The near-bottom flow also leads the near-surface flow; however, their

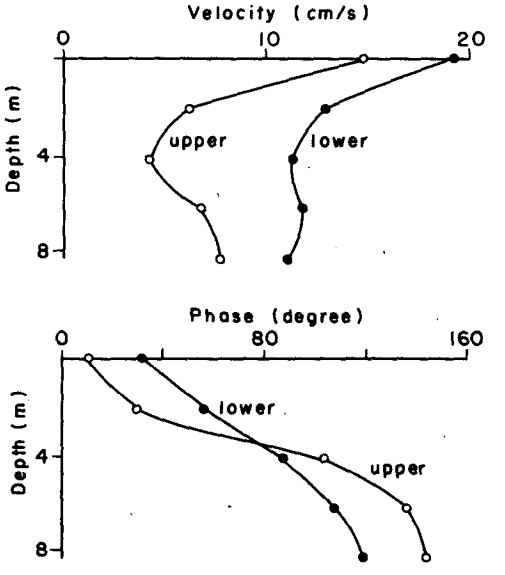

FIG. 6. The amplitude and phase of velocity in lower (50 km from the entrance) and upper (200 km from the entrance) Bay, from model computation. (A positive phase difference means phase lead, and the zero phase is referenced to the surface wind.)

phase difference is relatively small. Thus, velocities in the lower Bay are more or less barotropic, and they lead the wind by 80°.

The simple model indicates two unique features of the estuarine response to local wind forcing:

1) The response is baroclinic (frictional) in the upper Bay, and it is barotropic in the lower Bay.

2) The bottom current leads the surface current; the phase difference is large (over 90°) in the upper Bay.

Both results compare well with the observations. It should be pointed out that these results are rather insensitive to changes of the frictional parameters. An increased vertical eddy viscosity will decrease the near-surface velocity shear. And, an increased drag coefficient will increase the near-bottom velocity shear. Nevertheless, the response characteristics remain unchanged.

Nonlocal forcing due to changes of coastal sea level may also be modeled by Eqs. (1) and (2), with the boundary condition at the mouth being replaced by an oscillating surface elevation. The solutions indicate a linear decrease of transport toward the head. Velocities are homogeneous, with a slight decrease near the bottom. In other words, the response to coastal sea level change is barotropic throughout the Bay. This result is consistent with observations of a barotropic response during nonlocal events on 23–26 November and 7–10 December. (During the November event, the local wind was strong. Consequently, the near-surface current in the upper Bay was dominated by the frictional effect.)

4. Discussion

In a one-year study of the subtidal sea level variability, Wang (1979) found that at time scales of 2–3 days, large transport can be induced in the lower Bay by the local longitudinal wind. At longer time scales, Wang and Elliott (1978) also found evidence of large, coastal, wind-induced transport. The present study, based on direct current measurements, provides further evidence of large, wind-driven, barotropic fluctuations in the lower Bay.

In the upper Bay, the response to wind forcing had a large baroclinic component. The nearsurface current was frictionally driven by the local wind, while the near-bottom current reflected effects of the large-scale motion. Similar results were also found in a recent, more extensive study (Grano and Pritchard, 1978). In contrast, Elliott *et al.* (1978) found a predominant barotropic response near the head of the Bay (40 km north of the upper Bay mooring location).

A simple frictional model is constructed to examine the nature of estuarine response. There are two basic driving mechanisms: the depth-independent slope effect and the frictional (shear stress) effect. In the upper Bay, the near-surface windstress is dominant, which results in a frictional response. The windstress effect is reduced towards the mouth, due to the opposing, increased interior dissipation (associated with the increased transport). Consequently, the slope effect becomes dominant in the lower Bay which results in a barotropic response. We have also examined the estuarine response to changes in coastal sea level (nonlocal forcing), and found the response basically barotropic.

The frictional model compares well with the observations. It offers a simple explanation for differences in the response between the lower and upper Bay. It also predicts the large vertical phase propagation, which is a characteristic feature of the wind-driven circulation. The apparent inconsistent result of Elliott *et al.* (1978) is probably due to the dominance of coastal sea level effect during the particular study.

The density effect is not included (explicitly) in the frictional model, which does not imply that density is not important in the estuarine response. The vertical eddy viscosity will certainly depend on the stratification. A strong stratification tends to reduce the vertical eddy viscosity, and hence it will support a larger near-surface shear. In contrast, a weak stratification will favor a barotropic response. Similarly, the interior dissipation can also be affected by the stratification. However, we do not have enough information to make even a qualitative estimation.

Because the salt fluxes associated with velocity fluctuations are large, the stratification may change significantly over a wind event. Consequently, the gravitational (density-induced) circulation can also be affected by the wind forcing. Tentative evidence for wind-induced change in gravitational circulation was found in the lower Bay. At the beginning of the current meter study, the vertical shears (between 13 and 26 ft) were small (Fig. 3). However, they increased significantly on 26 November and persisted afterward (during the period of common records). As the several-day fluctuations were mainly barotropic in the lower Bay, the slow-varying vertical shears were an indication of the strength of gravitational circulation. The sudden buildup of vertical shears, and hence, the gravitational circulation on 26 November, appeared to be the result of the preceeding, strong inflow event, when velocities were landward at all depths. Perhaps the increased salinities enhanced the gravitational circulation.

In conclusion, our study indicates large, atmospherically induced exchange between the Chesapeake Bay and coastal ocean. It also suggests

interaction between the wind-driven and density-induced circulation. Since knowledge of upstream salt intrusion is of great practical importance, relations between the horizontal circulation and salinity distribution need further quantitative examination.

Acknowledgments. I am indebted to Dr. A. J. Elliott who originally conducted the current measurement study. Dr. C. N. K. Mooers and an anonymous reviewer made many helpful comments, particularly regarding model interpretation. This study was supported by the National Science Foundation as part of Grants OCE 74-08463 and OCE 77-20254.

REFERENCES

Elliott, A. J., 1978: Observations of the meteorologically induced circulation in the Potomac estuary. *Estuarine Coastal Mar. Sci.*, **6**, 285–300.

——, D-P Wang and D. W. Pritchard, 1978: The circulation near the head of Chesapeake Bay. *J. Mar. Res.*, **36**, 643–655.

Grano, V., and D. W. Pritchard, 1978: Wind-driven, nontidal circulation of the upper Chesapeake Bay. *Trans. Amer. Geophys. Union.*, **50**, 1102.

Pritchard, D. W., 1952: Salinity distribution and circulation in the Chesapeake Bay estuarine system. *J. Mar. Res.*, **11**, 106–123.

——, 1956: The dynamic structure of a coastal plain estuary. *J. Mar. Res.*, **15**, 33–42.

Smith, N. P., 1977: Meteorological and tidal exchanges between Corpus Christi Bay, Texas, and the northwestern Gulf of Mexico. *Estuarine Coastal Mar. Sci.*, **5**, 511–520.

Wang, D-P., 1979: Subtidal sea level variations in the Chesapeake Bay and relations to atmospheric forcing. *J. Phys. Oceanogr.*, **9**, 413–421.

——, and A. J. Elliott, 1978: Nontidal variability in the Chesapeake Bay and Potomac River: Evidence for nonlocal forcing. *J. Phys. Oceanogr.*, **8**, 225–232.

Weisberg, R. H., 1976: The nontidal flow in the Providence River of Narragansett Bay: A stochastic approach to estuarine circulation. *J. Phys. Oceanogr.*, **6**, 721–734.